The Canadian Mineralogist
Vol. 56, pp. 365-373 (2018)
DOI: 10.3749/canmin.1800015

SPECTROSCOPIC CHARACTERIZATION AND THERMAL RECRYSTALLIZATION STUDY OF AN UNKNOWN METAMICT PHASE FROM TUFTEN QUARRY, SOUTHERN NORWAY

DARIUSZ MALCZEWSKI[§], MARIA DZIUROWICZ, AND TOMASZ KRZYKAWSKI

Faculty of Earth Sciences, University of Silesia, Bedzinska 60, 41-200 Sosnowiec, Poland

AGNIESZKA GRABIAS

Institute of Electronic Materials Technology, Wolczynska 133, 01-919 Warszawa, Poland

ABSTRACT

This paper presents the results of ^{57}Fe Mössbauer spectroscopy, SEM-EDS analysis, gamma-ray spectrometry, and X-ray diffraction (XRD) patterns for an unknown metamict phase (UMP) from a syenite pegmatite at Tuften quarry, southern Norway. The sample exhibits ^{232}Th and ^{238}U activities of 137 and 2.6 Bq g^{-1}, respectively, and a calculated total absorbed α-dose of 8×10^{15} α-decay mg^{-1}. Its chemical composition falls generally between chevkinite-(Ce)–perrierite-(Ce) and allanite-(Ce)–ferriallanite-(Ce) mineral compositions. The Mössbauer spectrum of an untreated UMP sample can be fitted to two Fe^{2+} and Fe^{3+} quadrupole doublets assigned to octahedral coordination with a relative $Fe^{2+}/\Sigma Fe$ ratio of 0.11. A sample of the UMP was also annealed in argon for one hour at 1273 K. Powder of the completely recrystallized sample was subjected to XRD analysis and indexed to the *P*121 space group with unit-cell dimensions of *a* 8.179 Å, *b* 14.16 Å, *c* 4.291 Å, and $\beta = 96.71°$. The corresponding Mössbauer spectrum is characterized by the presence of three quadrupole doublets also assigned to Fe^{2+} and Fe^{3+} in octahedral coordination with a relative $Fe^{2+}/\Sigma Fe$ ratio of 0.15. One of the Fe^{3+} doublets shows extremely high quadrupole splitting of 2.60 mm s^{-1}, implying extreme distortion of the coordination octahedra.

Keywords: unknown metamict phase, syenite pegmatite, alpha-doses, gamma-ray spectrometry, X-ray diffraction, Mössbauer spectroscopy.

INTRODUCTION

Metamict minerals are a class of natural, amorphous materials whose original crystalline structure is degraded by internal radioactive decay over geologic time. Damage in these phases is mainly caused by recoil nuclei from α-decay of ^{238}U, ^{232}Th, ^{235}U, and their daughter products. Loss of crystal morphology and structure can obscure the original mineral phase. The original crystalline structure of a metamict mineral may be restored with high-temperature annealing in the presence of an inert gas. These minerals are widely used in geochronology due to the natural incorporation of uranium and thorium as trace or major constituents in their mineral matrix (Meldrum *et al*. 1998).

A black, brittle, vitreous sample (Fig. 1) of an unknown metamict phase (UMP) was collected from a pegmatite at Tuften quarry situated in the Langensundfjord area of southern Norway. The pegmatite has been dated at 293.2(13) Ma (Dahlgren *et al*. 1998, Müller *et al*. 2017). The Tuften quarry is one of several actively used sources of larvikite (a local name for alkali syenite or monzonite) and is associated with the Permian-aged Larvik Plutonic Complex (LPC) of the southern part of the Oslo Graben (Petersen 1978, Pedersen *et al*. 1995, Andersen *et al*. 2013). The LPC is characterized by relatively large syenite and nepheline syenite pegmatites. Dikes of 1 m thickness are common while some dikes attain thicknesses of 10–20 m and 120 m length (Müller *et al*. 2017). To date, as many as 227 different minerals have been

§ *Corresponding author e-mail address*: dariusz.malczewski@us.edu.pl

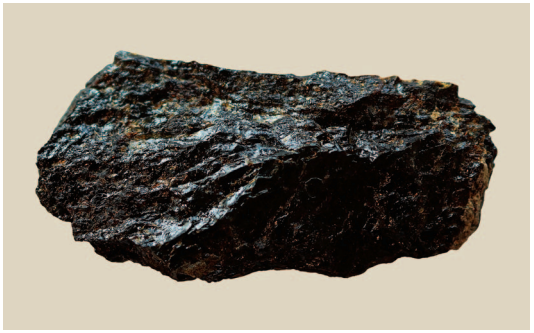

FIG. 1. Photo of the unknown metamict phase (UMP); 2.5 cm in length (photo by D. Malczewski). This specimen is characterized by ^{232}Th and ^{238}U activities of 136.6 Bq g^{-1} and 2.64 Bq g^{-1}, respectively.

identified as occurring in the Larvik Plutonic Complex (LPC) pegmatites (Piilonen *et al*. 2013, Larsen 2017). More than 100 of these occur in the AS Granit and Tuften larvikite quarries at Tvedalen, Larvik, and Vestfold. A comprehensive list of minerals found in the LPC is maintained and updated as new phases are identified (Grice *et al*. 2013, Friis *et al*. 2014, 2017, Sokolova *et al*. 2017). This list consists of major minerals and numerous rare minerals, including economically important phases such as those enriched in REE, Be, and F (Müller *et al*. 2017).

This study presents basic spectroscopic data for an unknown metamict phase (UMP) (Fig. 2) and partially interprets its original crystalline structure following high-temperature annealing in argon.

MATERIALS AND METHODS

The chemical composition of the UMP sample was obtained using a JEOL JSM-6480 scanning electron microscope with an energy dispersive X-ray spectrometer (SEM-EDS) operated at an accelerating voltage of 20 kV and 30 μA current. Elemental compositions were interpreted using EDS2006 software. The electron-microprobe data were collected from 10 grains of the UMP sample. Table 1 gives the chemical composition, calculated α-doses, and radon (^{222}Rn) and thoron (^{220}Rn) emanation coefficients.

Concentrations of ^{238}U and ^{232}Th were calculated based on the gamma-ray activities of ^{214}Pb and ^{214}Bi for ^{238}U and of ^{228}Ac for ^{232}Th. Gamma-ray spectra were collected using a GX4018 system consisting of a coaxial HPGe detector (45.2% efficiency) in a lead and copper shield (102 mm) with a Lynx multichannel buffer. Radionuclide activities were calculated from the following gamma transitions: ^{214}Pb (241.9, 295.2, and 351.9 keV), ^{214}Bi (609.3, 768.3, 1120.3, and 1764.5 keV), and ^{228}Ac (338.3, 911.6, 964.6, and 969.1 keV). LabSOCS (Laboratory Sourceless Calibration Software) and Genie 2000 v.3.4 software

TABLE 1. CHEMICAL COMPOSITION, ^{222}Rn and ^{220}Rn EMANATION COEFFICIENTS, DENSITY, AND CALCULATED α-DOSES OF THE UNKNOWN METAMICT PHASE (UMP) EXAMINED IN THIS STUDY

O	27.9(45)
Al	5.4(12)
Si	9.3(18)
Ca	5.0(7)
Ti	0.5(2)
Fe	3.3(5)
Ge	0.5(3)
Se	1.2(7)
Rb	1.0(7)
Y	3.6(12)
Te	2.2(7)
La	2.8(9)
Ce	11.9(23)
Nd	2.9(9)
Σ Pr-Lu	9.3(19)
Ta	1.6(9)
W	1.5(8)
Pb	4.7(18)
Th	3.36(3)
U	0.020(1)
Total	97.98
D (calc)	4.54 g cm^{-3}
D (obs)	3.80 g cm^{-3}
Calculated total dose (D_T)[a] (α-decay mg^{-1})	7.89(8) × 10^{15}
Calculated dose from ^{232}Th (D_{232}) (α-decay mg^{-1})	7.68(7) × 10^{15}
Calculated dose from ^{238}U (D_{238}) (α-decay mg^{-1})	1.97(15) × 10^{14}
Calculated dose from ^{235}U (D_{235}) (α-decay mg^{-1})	9.1(7) × 10^{12}
e_{222}[b]	0.009%
e_{220}	0.01%

[a] Doses were calculated as: $D_{238} = 8 \times N_{238}(e^{t\lambda.238} - 1)$, $D_{235} = 7 \times N_{235}(e^{t\lambda.235} - 1)$, $D_{232} = 6 \times N_{232}(e^{t\lambda.232} - 1)$, and $D_T = D_{238} + D_{235} + D_{232}$. N_{238}, N_{235}, and N_{232} are the present number of atoms of ^{238}U, ^{235}U, and ^{232}Th per milligram, λ_{238}, λ_{235}, and λ_{232} are the decay constants of ^{238}U, ^{235}U, and ^{232}Th (respectively), and t is the geologic age. The absorbed ^{235}U α-doses were calculated assuming a natural atomic abundance of ^{238}U/^{235}U = 137.88.

[b] ^{222}Rn emanation coefficient (e_{222}) and ^{220}Rn emanation coefficient (e_{220}).

TABLE 2. HYPERFINE ^{57}Fe MÖSSBAUER SPECTRAL PARAMETERS FOR UNTREATED UMP SAMPLE (FIG. 3) FROM TUFTEN QUARRY (ISOMER SHIFT VALUES (IS) ARE GIVEN RELATIVE TO THE α-Fe STANDARD)

Doublet no.	Assignment (CN)[a]	χ^2	IS (mm s^{-1})	QS (mm s^{-1})	Γ [b] (mm s^{-1})	Intensity
1	Fe^{2+} (6)	1.9	1.18(1)	2.27(1)	0.21(2)	0.11(1)
2	Fe^{3+} (6)		0.35(1)	0.82(1)	0.31(1)	0.89(1)

[a] CN = coordination number.
[b] Half-width at half-maximum.

packages were used to calibrate efficiency and determine radionuclides and their activities.

After splitting the sample into fragments, the pieces were placed in quartz tubes, sealed under argon, and annealed for one hour in a muffle furnace at 673, 873, 1073, 1173, and 1273 K. Each temperature was stabilized at ±2 K. After annealing, the samples were quenched and ground into powder.

The annealed UMP fragments were analyzed for their X-ray diffraction (XRD) patterns with a PANalytical XPert PRO MPD diffractometer using Θ-Θ geometry and Cu*K*α radiation in the scan mode with a step size of 0.02° and processing with HIGHSCORE+ Panalytical v.4.6 software (Degen *et al*. 2014). The Dicvol 06 indexing software, optimized for monoclinic and triclinic structures, was used to search for prospective unit cells (Boultif & Louër 1991, 2004, Louër & Boultif 2007).

For ^{57}Fe Mössbauer spectroscopy the powder samples were mounted as a thin disc absorber. Mössbauer transmission spectra of the untreated UMP sample and a fragment annealed at 1273 K were recorded at room temperature using a constant acceleration spectrometer, a multichannel analyzer with 512 channels, and a linear arrangement of a ^{57}Co/Rh source (= 50 mCi) absorber and detector. Mössbauer spectra were numerically analyzed using Recoil and MEP fitting software.

A RAD7 radon system was used to measure emanation coefficients e_{222}(%) and e_{220}(%) (Table 1) of ^{222}Rn and ^{220}Rn isotopes, respectively. Detailed description of RAD7 electronics and measurement configuration are provided by Durridge Company Inc. (2000) and Malczewski & Dziurowicz (2015).

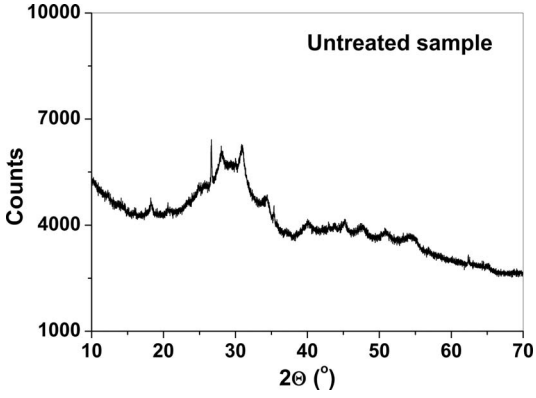

FIG. 2. XRD pattern of an untreated UMP fragment.

RESULTS AND DISCUSSION

The chemical composition of the UMP specimen (Table 1) generally resembles that of chevkinite-(Ce) $[(Ce,La,Ca,Th)_4Fe^{2+}(Ti,Fe^{3+},Nb)_4Si_4O_{22}]$ – perrierite-(Ce) $[(Ce,La,Ca)_4(Fe^{2+},Mg)(Ti,Fe^{3+})_3Si_4O_{22}]$ minerals but with significantly higher Al, Pb, and Y concentrations and significantly lower Ti concentrations (~0.54 wt.%) relative to those of chevkinite and perrierite (Gottardi 1960, Mitchell 1966, Segalstad & Larsen 1978, Calvo & Faggiani 1974, Parodi *et al*. 1994, Sokolova *et al*. 2004). The UMP chemical composition also resembles that of allanite-(Ce) $[(Ce,Ca,Y)_2(Al,Fe)_3(SiO_4)_3OH]$ – ferriallanite-(Ce)

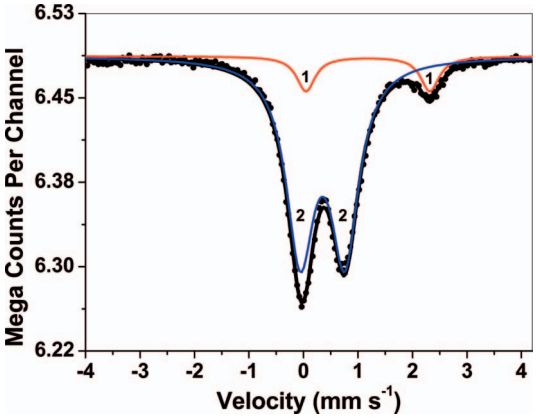

FIG. 3. ^{57}Fe Mössbauer spectrum of an untreated UMP sample. Solid dots – experimental data; thick solid line – fitted curve; thin solid line – fitted doublets: 1 = Fe^{2+}, 2 = Fe^{3+}.

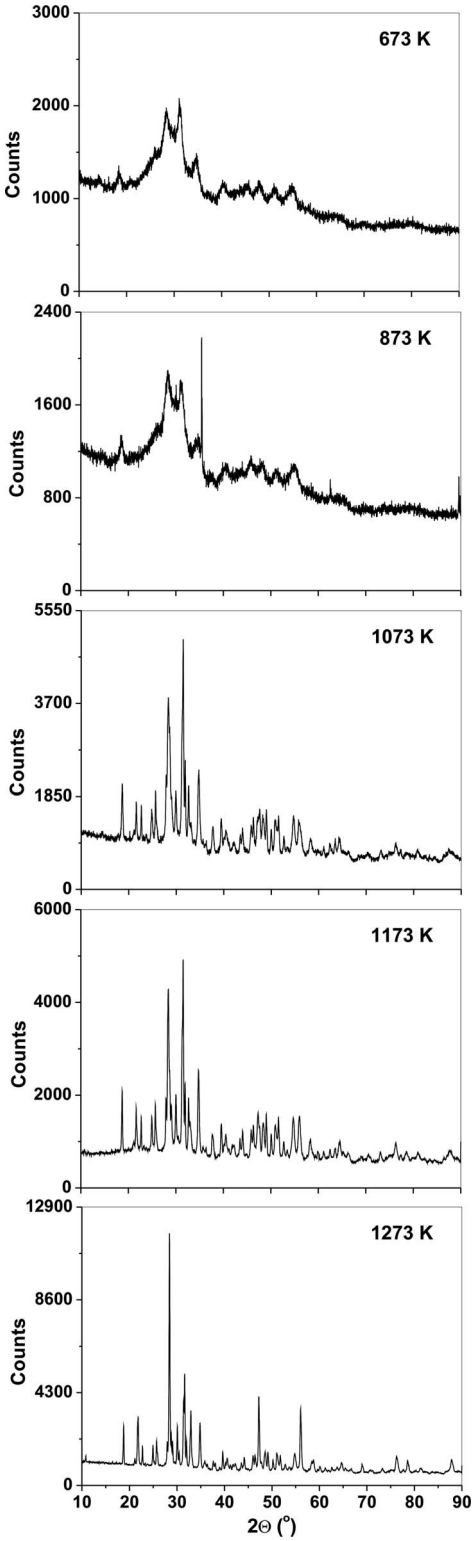

[$CaCe(Fe,Al)_3(SiO_4)(Si_2O_7)O(OH)$] (Dollase 1971, Kartashov *et al*. 2002).

The ^{57}Fe Mössbauer spectrum of an untreated UMP fragment included two quadrupole doublets representing Fe^{2+} and Fe^{3+} (Table 2, Fig. 3). The first doublet (no. 1, Fig. 3) exhibited an IS (isomer shift) value of 1.18 mm s^{-1} and a QS (quadrupole splitting) value of 2.27 mm s^{-1}, which correspond to Fe^{2+} in octahedral coordination. The doublet labeled no. 2 exhibited an IS value of 0.35 mm s^{-1} and a QS value of 0.82 mm s^{-1}, which correspond to Fe^{3+}, also in octahedral coordination. The relative areas of these doublets are 0.11 and 0.89, giving a relative, divalent iron ($Fe^{2+}/\Sigma Fe$) contribution of 11% for the untreated UMP sample. Both IS and QS values for the Fe^{2+} and Fe^{3+} components indicate that the coordinated octahedra are regular (Ingalls 1964, Hawthorne 1988).

In the only known paper describing Mössbauer spectroscopy of metamict chevkinite, Li *et al*. (1992) reported similar values for hyperfine parameters. These workers specifically reported average IS and QS values of 1.19 and 0.38 mm s^{-1} for Fe^{2+} and 2.23 and 0.95 mm s^{-1} for Fe^{3+}, respectively. The Fe^{2+} contribution, however, attained values as high as 0.43. The authors did not describe the degree of metamictization of the sample investigated, but fitted line widths suggest that the sample was partially metamict.

Annealing path

Figure 4 shows XRD diffraction patterns for UMP fragments after one hour of annealing in argon at 673, 873, 1073, 1173, and 1273 K. As seen in this Figure, the sample recrystallized with increasing temperature, and the sample annealed at 1273 K appears completely crystalline. Table 3 lists XRD powder data along with indexing of the reflections. After processing XRD data, the best fit was obtained for the *P*121 space group with the cell parameters presented in Table 4. Figure 5 shows the high degree of agreement between experimental XRD patterns and those calculated for the *P*121 space group. ICSD (2015) and ICDD PDF4+ (2017) diffraction data bases did not return a matching silicate phase for the indexed peaks listed in Table 3. As seen in Table 5, the unit-cell parameters of the annealed UMP sample differ significantly from those reported for allanite, ferriallanite, chevkinite, gadolinite, and perrierite. The data reveal similarities in the "*a*" lattice constant and in unit cell volume for allanite, ferriallanite, and the UMP sample.

←

FIG. 4. XRD patterns for UMP fragments annealed in argon at the given temperatures.

TABLE 3. XRD POWDER DATA FOR THE UMP SAMPLE ANNEALED AT 1273 K IN ARGON (Cu$K\alpha$ RADIATION)

No.	Position 2θ (°)	*d*-spacing (Å)	Relative int. (%)	*h*	*k*	*l*
1	10.834	8.166	3.62	1	0	0
2	18.753	4.728	15.86	0	3	0
3	21.119	4.203	2.27	0	0	1
4	21.688	4.094	12.27	1	3	0
5	21.825	4.069	15.77	2	0	0
6	22.738	3.908	8.84	2	1	0
7	24.935	3.568	8.61	1	0	1
8	25.227	3.527	1.66	2	2	0
9	25.702	3.463	10.77	1	1	1
10	25.914	3.436	4.08	1	2	$\bar{1}$
11	27.928	3.192	8.25	1	2	1
12	28.403	3.140	100	0	3	1
13	28.796	3.098	9.86	2	0	$\bar{1}$
14	29.053	3.071	9.85	2	3	0
15	30.055	2.971	18	1	3	$\bar{1}$
16	30.440	2.934	5.79	-	-	-
17	31.383	2.848	26.65	2	2	$\bar{1}$
18	31.611	2.828	40.5	0	5	0
19	31.981	2.796	10.36	-	-	-
20	32.849	2.724	11.68	-	-	-
21	32.930	2.718	13.79	2	1	1
22	34.819	2.575	18.92	2	2	1
23	35.846	2.503	3.5	1	4	1
24	36.343	2.470	1.48	-	-	-
25	37.635	2.388	3.93	2	3	1
26	38.028	2.364	2.89	0	6	0
27	38.966	2.310	1.64	2	5	0
28	39.622	2.273	8.72	3	2	$\bar{1}$
29	40.229	2.240	2.36	-	-	-
30	40.568	2.222	4.63	1	5	1
31	41.232	2.188	2.2	2	4	1
32	41.786	2.160	2.08	3	0	1
33	42.252	2.137	2.58	3	1	1
34	43.549	2.077	3.43	0	1	$\bar{2}$
35	44.150	2.050	6	0	6	$\bar{1}$
36	45.984	1.972	6.06	1	0	2
37	46.436	1.954	6.17	1	1	2
38	47.225	1.923	34.26	4	0	$\bar{1}$
39	47.754	1.903	2.53	1	2	2
40	48.522	1.875	7.39	2	6	$\bar{1}$
41	49.134	1.853	8.9	4	2	$\bar{1}$
42	50.201	1.816	5.45	2	7	0
43	51.023	1.789	7.69	2	6	1
44	51.247	1.781	2.67	3	6	0
45	51.734	1.766	6.62	2	1	2
46	52.759	1.734	2.76	4	1	1
47	53.619	1.708	1.25	3	2	$\bar{2}$
48	54.766	1.675	6.73	1	5	$\bar{2}$
49	56.023	1.640	29.65	4	3	1
50	58.342	1.580	4.07	5	0	$\bar{1}$
51	58.730	1.571	4.25	3	0	2
52	60.074	1.539	2.44	4	6	0
53	61.228	1.513	1.58	1	6	2
54	62.604	1.483	1.98	3	8	0
55	63.674	1.460	1.89	1	9	$\bar{1}$
56	64.621	1.441	3.92	5	4	$\bar{1}$
57	65.458	1.425	1.79	3	8	$\bar{1}$
58	66.518	1.405	1.22	1	0	$\bar{3}$
59	68.987	1.360	4.2	3	9	0
60	70.628	1.333	1.31	1	10	$\bar{1}$
61	71.176	1.324	0.78	4	7	1
62	73.195	1.292	1.85	2	10	$\bar{1}$
63	75.057	1.265	1.18	6	4	0
64	76.183	1.249	7	6	4	$\bar{1}$
65	76.482	1.244	2.24	5	7	$\bar{1}$
66	77.574	1.230	1.35	1	9	2
67	78.545	1.217	6.18	5	0	2
68	80.139	1.197	0.91	5	8	0
69	81.300	1.182	2.26	3	1	3
70	81.609	1.180	2.21	2	9	2
71	82.341	1.170	0.55	4	9	1
72	83.714	1.154	0.64	1	7	$\bar{3}$
73	84.770	1.143	0.59	3	6	$\bar{3}$
74	86.965	1.119	0.83	4	5	$\bar{3}$
75	87.795	1.111	6.48	3	9	2

As shown in Figure 6, the Mössbauer spectrum of a UMP fragment annealed at 1273 K in argon represents a superposition of three quadrupole doublets assigned to Fe^{2+} (no. 1) and Fe^{3+} (nos. 2 and 3). Based on IS values (Hawthorne 1988), all of the doublets represent iron ions in octahedral coordination (Table 6). The Fe^{2+} component is characterized by an IS of 1.04 mm s^{-1} and a QS of 1.73 mm s^{-1} with a relative area of 0.15. This indicates an increase in the relative contribution of divalent iron ($Fe^{2+}/\Sigma Fe = 15\%$)

TABLE 4. UNIT-CELL DIMENSIONS CALCULATED FOR THE UMP PHASE AFTER ANNEALING AT 1273 K IN ARGON

Name	Value
Space group	*P*121
a (Å)	8.179(6)
b (Å)	14.16(1)
c (Å)	4.219(3)
α (°)	90
β (°)	96.71(1)
γ (°)	90
V (Å^3)	485.3

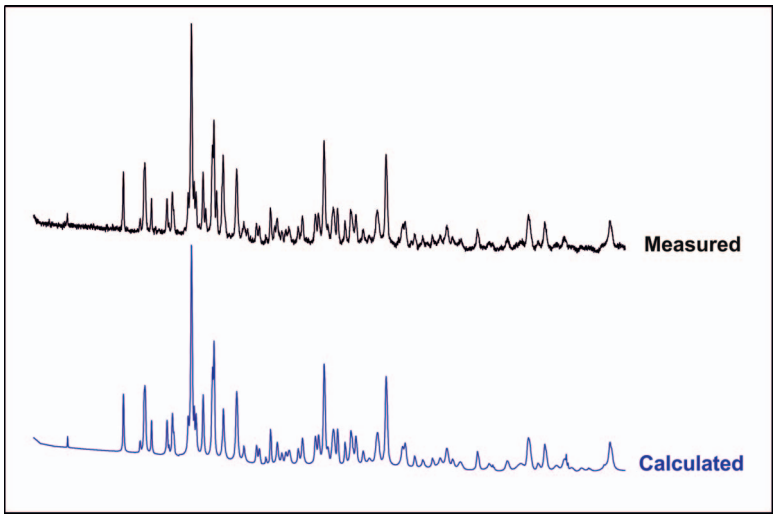

FIG. 5. Comparison of XRD patterns for a sample annealed at 1273 K for one hour (above) and a calculated XRD pattern for the *P*121 space group (below).

relative to that observed for the untreated sample (Fig. 3, Table 2). The spectrum is dominated by extremely large quadrupole doublets (no. 2) for Fe^{3+} having a QS value of 2.53 mm s^{-1} (Table 6). Such large Fe^{3+} doublets have only been observed in gadolinite-(Ca) [$CaREE_2Fe^{3+}Be_2(Si_2O_{10})$] and gadolinite-(Y) [$REE_2Fe^{2+}Be_2(Si_2O_{10})$] (Ito & Hafner 1974, Malczewski 2010). Samples of crystalline and partially metamict allanites also contained Fe^{3+} doublets with comparable QS values of 2–2.30 mm s^{-1} (Dollase 1971, Malczewski & Grabias 2008b). In crystalline and partially metamict gadolinite the central iron and oxygen ions form a highly distorted octahedron with an average Fe–O distance of 2.18 Å, a value which approaches the sum of the ionic radii of Fe^{2+} and O^{2-}, estimated to be between 2.16 and 2.18 Å (Miyawaki *et al*. 1984). The octahedron shows the Jahn-Teller effect and bond lengths of apex oxygens, Fe–(O5, O5′) of 2.04 Å, are shorter than the others. The iron octahedron in the crystalline state of the UMP sample exhibits a similar geometry.

Hyperfine parameters for the Fe^{3+} doublet (no. 2) combined with low Fe^{2+} doublet values for both IS and QS (no. 1) indicate that Fe^{2+} and Fe^{3+} ions occupy the same cation site. Fe^{2+} and Fe^{3+} share the M(1) or B site in chevkinite–perrierite minerals (Segalstad & Larsen 1978, Parodi *et al*. 1994, Sokolova *et al*. 2004), the M(3) site in allanite (Dollase 1971), and the only Fe site in gadolinite (Miyawaki *et al*. 1984). Fe^{2+} and Fe^{3+} doublets representing divalent and trivalent iron at a similar site with highly distorted octahedral coordination have been observed from crystalline and

TABLE 5. COMPARISON OF CRYSTAL DATA FOR ALLANITE, CHEVKINITE, FERRIALLANITE, GADOLINITE, PERRIERITE, AND THE ANNEALED UMP SAMPLE

Name	Allanite-(Ce)[a]	Chevkinite-(Ce)[b]	Ferriallanite-(Ce)[c]	Gadolinite-(Y)[d]	Perrierite-(Ce)[e]	UMP
Crystal system	monoclinic	monoclinic	monoclinic	monoclinic	monoclinic	monoclinic
Space group	$P2_1/m$	$C2/m$	$P2_1/m$	$P2_1/a$	$P2_1/m$	$P121$
a (Å)	8.927	13.400	8.962	10.000	13.629	8.179
b (Å)	5.761	5.7232	5.836	7.565	5.727	14.16
c (Å)	10.150	11.0573	10.182	4.768	11.715	4.219
β (°)	114.77	100.537	115.02	90.31	113.74	96.71
V (Å^3)	474.0	833.7	482.6	360.7	835.5	485.3

[a] Dollase (1971); [b] Sokolova *et al.* (2004); [c] Kartashov *et al.* (2002); [d] Miyawaki *et al.* (1984); [e] Parodi *et al.* (1994).

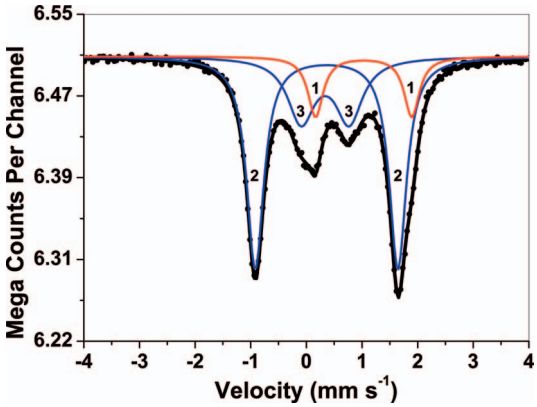

FIG. 6. ^{57}Fe Mössbauer spectrum for the UMP after annealing at 1273 K. Solid dots – experimental data; thick solid line – fitted curve; thin solid line – fitted doublets: 1 = Fe^{2+}, 2 = Fe^{3+}, 3 = Fe^{3+}.

partially metamict gadolinites (Ito & Hafner 1974, Malczewski 2010). These doublets also appear, albeit with somewhat lower Fe^{3+} QS values, in partially metamict cerite and perrierite (Malczewski & Grabias 2008a).

The second doublet assigned to Fe^{3+} (no. 3, Fig. 6, Table 6) has a relative area of 0.27. The Mössbauer parameters of this doublet (IS = 0.34 mm s^{-1} and QS = 0.86 mm s^{-1}) suggest a regular environment. This Fe^{3+} position may correspond to the M(2) site in chevkinite or C site in perrierite and the M(1) site in allanite or M(2) site in ferriallanite.

The data indicate that in the UMP's crystalline state, Fe ions occur mainly as Fe^{3+}, while the relative Fe^{2+} contribution does not exceed 20%. The sample's Mössbauer spectrum differs markedly from those reported for samples of allanite, ferriallanite, chevkinite, and perrierite, despite close similarities in chemical composition and crystal structure.

CONCLUSIONS

Results of the spectroscopic study of a fully metamict thorium-bearing UMP sample from the Tuften quarry suggest that this specimen is a new phase among rare earth silicates with a monoclinic structure resembling those of allanite, ferriallanite, chevkinite, or perrierite. Mössbauer spectra collected following sample annealing at 1273 K in argon can be fitted to three quadrupole doublets representing Fe^{2+} and Fe^{3+} at two different octahedrally coordinated sites. One of the sites may be interpreted as being occupied by both Fe^{2+} and Fe^{3+} with highly distorted octahedral coordination, whereas the second represents Fe^{3+} occupation with less distorted or regular octahedral coordination.

ACKNOWLEDGMENTS

This work was supported by the National Science Centre, Poland, through grant No. 2014/15/B/ST10/04095. The authors sincerely thank Ingulv Burvald, a Norwegian private mineral collector, for providing the mineral sample for this study. We also thank the Leading National Research Centre (KNOW) of the Centre for Polar Study of the University of Silesia, Faculty of Earth Sciences, Poland, for financial support, which allowed the authors to take part in the 2017 PEG Symposium in Norway.

TABLE 6. HYPERFINE ^{57}Fe MÖSSBAUER SPECTRAL PARAMETERS FOR THE UMP SAMPLE ANNEALED AT 1273 K IN ARGON (FIG. 6) (ISOMER SHIFT VALUES (IS) ARE GIVEN RELATIVE TO THE α-Fe STANDARD)

Doublet no.	Assignment (CN)[a]	χ^2	IS (mm s^{-1})	QS (mm s^{-1})	Γ [b] (mm s^{-1})	Intensity
1	Fe^{2+} (6)	1.2	1.03(1)	1.73(1)	0.16(1)	0.15(1)
2	Fe^{3+} (6)		0.36(1)	2.56(1)	0.19(1)	0.58(1)
3	Fe^{3+} (6)		0.34(1)	0.86(1)	0.29(1)	0.27(1)

[a] CN = coordination number; [b] Half-width at half-maximum.

References

Andersen, T., Erambert, M., Larsen, A.O., & Selbekk, R.S. (2013) Petrology of nepheline syenite pegmatites in the Oslo Rift, Norway: Zr and Ti mineral assemblages in miaskitic and agpaitic pegmatites in the Larvik Plutonic Complex. *Mineralogia* **44(3–4)**, 61–98.

Boultif, A. & Louër, D. (1991) Indexing of powder diffraction patterns for low-symmetry lattices by the successive dichotomy method. *Journal of Applied Crystallography* **24**, 987–993.

Boultif, A. & Louër, D. (2004) Powder pattern indexing with the dichotomy method. *Journal of Applied Crystallography* **37**, 724–731.

Calvo, C. & Faggiani, R. (1974) A re-investigation of the crystal structures of chevkinite and perrierite. *American Mineralogist* **59**, 1277–1285.

Dahlgren, S., Corfu, F., & Heaman, L. (1998) Datering av plutoner og pegmatitter i Larvik pluton-kompleks, sydlige Oslo Graben, ved hjelp av U-Pb isotoper i zirkon og baddeleyitt. Kongsberg Mineralsymposium, *Norsk Bergverksmuseum Skrift* **14**, 32–39.

Degen, T., Sadki, M., Bron, E., König, U., & Nenert, G. (2014) The HighScore suite. *Powder Diffraction* (Supplement S2) **29**, S13–S18.

Dollase, W.A. (1971) Refinement of the crystal structures of epidote, allanite and hancockite. *American Mineralogist* **56**, 447–464.

Durridge Company Inc. (2000) *RAD7 Radon Detector*. Part No. 1280, Durridge Company Inc., Bedford, Massachuests.

Friis, H., Larsen, A.O., Kampf, A.R., Evans, R.J., Selbekk, R.S., Sánchez, A.A., & Kihle, J. (2014) Peterandresenite, $Mn_4Nb_6O_{19}{\cdot}14H_2O$, a new mineral containing the Linqvist ion from a syenite pegmatite of the Larvik Plutonic Complex, southern Norway. *European Journal of Mineralogy* **26**, 567–576.

Friis, H., Weller, M.T., & Kampf, A.R. (2017) Hansesmarkite, $Ca_2Mn_2Nb_6O_{19}{\cdot}2H_2O$, a new hexaniobate from a syenite pegmatite in the Larvik Plutonic Complex, southern Norway. *Mineralogical Magazine* **81(3)**, 543–554.

Gottardi, G. (1960) The crystal structure of perrierite. *American Mineralogist* **45**, 1–14.

Grice, J.D., Kristiansen, R., Friis, H., Rowe, R., Poirier, G.G., Selbekk, R.S., Cooper, M.A., & Larsen, A.O. (2013) Ferrochiavennite, a new beryllium silicate zeolite from syenite pegmatites in the Larvik Plutonic Complex, Oslo Region, Southern Norway. *Canadian Mineralogist* **51**, 285–296.

Hawthorne, F.C., Ed. (1988) Spectroscopic methods in mineralogy and geology. *Reviews in Mineralogy* **18**, 255–340.

Ingalls, R. (1964) Electric-field gradient tensor in ferrous compounds. *Physical Review* **133**, A787–A795.

Ito, J. & Hafner, S.S. (1974) Synthesis and study of gadolinites. *American Mineralogist* **59**, 700–708.

Kartashov, P.M., Ferraris, G., Ivaldi, G., Sokolova, E.V., & Mccammon, C.A. (2002) Ferriallanite-(Ce), $CaCeFe^{3+}AlFe^{2+}(SiO_4)(Si_2O_7)O(OH)$, a new member of the epidote group: description, X-ray and Mössbauer study. *Canadian Mineralogist* **40**, 1641–1648.

Larsen, K.E. (2017) List of minerals found in the Larvik Plutonic Complex. Available from: https://www.mindat.org/article.php/1747 [date accessed: 13th Aug 2017].

Li, Z., Jin, M., Liu, M., & Liu, X. (1992) Iron distribution in chevkinite. *Hyperfine Interactions* **70**, 1057–1060.

Louër, D. & Boultif, A. (2007) Powder pattern indexing and the dichotomy algorithm. *Zeitschrift für Kristallographie/Supplemente* **26**, 191–196.

Malczewski, D. (2010) Recrystallization in fully metamict gadolinite from Ytterby (Sweden), annealed in air and studied by ^{57}Fe Mössbauer spectroscopy. *American Mineralogist* **95**, 463–471.

Malczewski, D. & Dziurowicz, M. (2015) ^{222}Rn and ^{220}Rn emanations as a function of the absorbed alpha-doses from select metamict minerals. *American Mineralogist* **100**, 1378–1385.

Malczewski, D. & Grabias, A. (2008a) ^{57}Fe Mössbauer spectroscopy and X-ray diffraction study of complex metamict minerals. Part II. *Hyperfine Interact* **186**, 75–81.

Malczewski, D. & Grabias, A. (2008b) ^{57}Fe Mössbauer spectroscopy of radiation damaged allanites. *Acta Physica Polonica A* **114**, 1683–1690.

Meldrum, A., Boatner, L.A., Weber, W.J., & Ewing, R.C. (1998) Radiation damage in zircon and monazite. *Geochimica et Cosmochmica Acta* **62**, 2509–2520.

Mitchell, R.S. (1966) Virginia metamict minerals: perrierite and chevkenite. *American Mineralogist* **51**, 1394–1405.

Miyawaki, R., Nakai, I., & Nagashima, K. (1984) A refinement of the crystal structure of gadolinite. *American Mineralogist* **69**, 948–953.

Müller, A., Husdal, T., Øyvind, S., Friis, H., Andersen, T., Johansen, T.S., Werner, R., Øivind, T., & Olerud, S. (2017) Norwegian Pegmatites I: Tysfjord-Hamaroy, Evje-Iveland, Langensundsfjord. Geological Society of Norway, *NGF Geological Guides* **6-2017**.

Parodi, G.C., Della Ventura, G., Mottana, A., & Raudsepp, M. (1994) Zr-rich non metamict perrierite-(Ce) from holocrystalline ejecta in the Sabatini volcanic complex (Lathium, Italy). *Mineralogical Magazine* **58**, 607–613.

Pedersen, L.E., Heaman, L.M., & Holm, P.M. (1995) Further constraints on the temporal evolution of the Oslo Rift

from precise U-Pb zircon dating in the Siljan-Skrim area. *Lithos* **34**, 301–315.

Petersen, J.S. (1978) Structure of the Larvikite-Lardalite Complex, Oslo-Region, Norway, and its revolution. *Geologische Rundschau* **67**, 330–342.

Piilonen, P.C., McDonald, A.M., Poirier, G., Rowe, R., & Larsen, A.O. (2013) Mafic minerals of the alkaline pegmatites in the Larvik Plutonic Complex, Oslo Rift, southern Norway. *Canadian Mineralogist* **51**, 735–770.

Segalstad, T.V. & Larsen, A.O. (1978) Chevkinite and perrierite from the Oslo region, Norway. *American Mineralogist* **63**, 188–195.

Sokolova, E., Hawthorne, C., Della Ventura, G., & Kartashov, P.M. (2004) Chevkinite-(Ce): Crystal structure and the effect of moderate radiation-induced damage on site-occupancy refinement. *Canadian Mineralogist* **42**, 1013–1025.

Sokolova, E., Day, M.C., Hawthorne, F.C., & Kristiansen, R. (2017) Heyerdahlite, IMA 2016-108. CNMNC Newsletter No. 36, April 2017, page 407; *Mineralogical Magazine* **81**, 403–409.

Received February 15, 2018. Revised manuscript accepted May 29, 2018.